Journal of Information & Optimization Sciences
ISSN 0252-2667 (Print), ISSN 2169-0103 (Online)
Vol. 47 (2026), No. 3, pp. 1063–1084
DOI : 10.47974/JIOS-1876

Study on the molecular structure of hyaluronic acid conjugates using a new class of topological indices

Mohammad Hadi Akhbari
Department of Mathematics
Islamic Azad University
Estahban Branch
Estahban 7451864756
Iran

Abstract

Based on medical experiments, the molecular structure of drugs includes information about their physical-chemical properties. A theoretical descriptor tool for assessing these features is known as a topological index. In this study, the molecular structure of two anticancer drugs hyaluronic acid-Paclitaxel/Curcumin conjugates using an edge-division strategy in graph theory are evaluated. To ensure the correctness of calculations in this study, we use Mathematica and Matlab software. Several new invariants based on the vertex degree are computed for the molecular structures of ayaluronic acid conjugated with curcumin and paclitaxel. We obtain the exact values of these topological indices. The calculation of topological indices for these anticancer drugs provides a more comprehensive understanding of their molecular properties and biological behavior.

Subject Classification: *05C92, 05C09, 92E10.*

Keywords: *Hyaluronic acid, Cancer treatment, Paclitaxel, Curcumin, Topological indices, Sombor index.*

1. Introduction

The polymer-anticancer drug conjugates are the efficient approach to developing new drugs in cancer treatment [1]. Hyaluronic acid (HA) is an anionic natural polymer and has unique features such as biodegradable and chemically modifiable [2][3].

HA is naturally found within the extracellular matrix of many tissues and is extensively for improving targeted drug delivery [4]. Its molecular formula is $(C_{14}H_{21}NO_{11})_n$ (see Figure 1(a)).

ORCID-ID: **0000-0002-2669-4966**

E-mail: **hadi.akhbari@iau.ac.ir**

In general, HA and its conjugates can aid in overcoming the chemical agents of anticancer medications' poor water solubility and stability [5-7].

Paclitaxel (PTX) is one of well know anticancer drugs for the treatment of ovarian cancer, breast cancer, and other malignant tumors [8]. PTX has the molecular formula $C_{47}H_{51}NO_{14}$ the chemical structure is shown in Figure 1(b). Xin, Wang, and Xiang [9] presented that the conjugate of PTX with HA using amino acids between them has more stability in vivo conditions. Curcuma longa is a nutraceutical that has the important role as antineoplastic agent, an antifungal agent, a hepatoprotective agent, and an anti-inflammatory agent. Curcumin disrupts cell signal transduction by using different mechanisms such as inhibition of protein kinase C and can inhibit of tumor cell multiplication and tumor growth [10][11]. Since the water solubility of Curcumin is limited and its absorption in biological systems is poor, it is unsuitable for clinical practice [12]. Curcumin conjugates with hyaluronic acid are considered as a useful therapeutic approach to optimize tissue dispersion, extend curcumin release, and improve clinical results [6] (see Figure 1(c)). Because of the importance of derivatives of hyaluronic acid in anticancer drugs, the analysis of its molecular structure can be an effective role in those studies. The chemical, pharmacological, and biological properties of the chemical compounds and drugs can be investigated and predicated using topological indices as a well-known method of chemical graphs.

A subfield of mathematical chemistry is chemical graph theory which uses graph theory to model molecule structure and analyzes its chemical graph [13]. In such a way, the molecular structure is represented as a molecular graph with atoms as vertices and the bound (between the atoms). Topological indices are the numerical values related to the chemical structure that are used to explain the relationship between the chemical structure and numerous chemical characteristics [14] in the Quantitative Structure-Property Relationship (QSPR) studies to predict various properties [15][16].

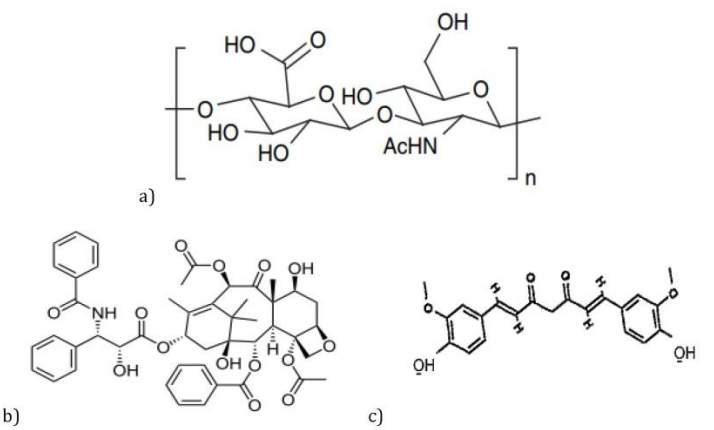

Figure 1
The molecular structure of a) Hyaluronic Acid, b) Paclitaxel, and c) Curcumin.

While researching alkane molecule boiling temperatures, Wiener [17] developed the idea of the topological index. Nowadays, numerous topological indices are introduced and studied on different molecular structures. For more studies on the topological indices and their applications, readers might refer to [18-26]. Topological Indices based on degree have been used in chemical engineering and pharmacology to investigate the structure of chemical compounds and drug properties.

Recently, many studies have been done on topological indices of the molecular graph of drugs. Rauf et al. [27] presented the results related to the EV-degree and the ve-degree-based topological indices for some molecular structures to study the pharmaceutical properties of drugs. In [28], some topological indices based on vertex degree of HA conjugated with curcumin are computed.

Mondal, De, and Pal [29] obtained some topological indices and neighborhood topological indices based on vertex degree using a polynomial approach for the drug treatment of COVID-19. Liu et al. [30] investigated the properties of various antiviral drugs including lopinavir, ritonavir, hydroxychloroquine, nafamostat, and camostat by using the distance in their molecular graph and bond measures.

Kirmani and Ali [31] analyzed the molecular graphs of HA-methotrexate/paclitaxel/curcumin conjugates to compute the topological coincides by applying CoM-polynomial. In [32], the structures of various COVID-19 drugs are analyzed to compute the CoM-polynomial and some degree-based topological coindices.

Throughout this paper, consider $G = (V_G, E_G)$ a molecular graph containing$|V_G| = n$ vertices and $|E_G| = m$ edges. loops. For two verities $y, w \in V_G$, if u and v are adjacent in G, then the edge joining between them is denoted by $e = yw$ where $e \in E$. The open neighborhood of $y \in V$ is $N_G(y) = \{w \in V_G : yw \in E_G\}$ and $|N_G(y)|$ is the degree of y and is denoted by $\xi(y)$.

Gutman [33] introduced a novel class of topological invariants based on Euclidian metric space with the geometric interpretation of the degree radius. The topological indices in this new class are called the Sombor index (SO),

$$SO(G) = \sum_{yw \in E_G} \sqrt{\xi(y)^2 + \xi(w)^2},$$

the reduced Sombor index (SO_{red}),

$$RSO(G) = SO_{red}(G) = \sum_{yw \in E_G} \sqrt{(\xi(y) - 1)^2 + (\xi(w) - 1)^2},$$

and the average Sombor index (SO_{avg}),

$$ASO(G) = SO_{avg}(G) = \sum_{yw \in E_G} \sqrt{\left(\xi(y) - \frac{2|E_G|}{|V_G|}\right)^2 + \left(\xi(w) - \frac{2|E_G|}{|V_G|}\right)^2}.$$

Various topological indices of a graph are presented with motivation of defining of the Sombor indices and well-known indices.

In [34], the authors defined the modified Sombor as follows

$$MSO(G) = \sum_{yw \in E_G} \frac{1}{\sqrt{\xi(y)^2 + \xi(w)^2}}.$$

They computed this index for certain chemical importance compounds [34].

In [35], the degree-based descriptors were extended by introducing multiplicative topological indices as follows

$$SOII(G) = \prod_{yw \in E_G} F\big(\xi(y), \xi(w)\big).$$

Due to much attention to calculation of the multiplicative indices of a graph and their applications, several multiplicative Sombor indices are definded including the multiplicative Sombor index (SOII) [36],

$$SOII(G) = \prod_{yw \in E_G} \sqrt{\xi(y)^2 + \xi(w)^2},$$

the multiplicative modified Sombor index (MSOII),

$$MSOII(G) = \prod_{yw \in E_G} \frac{1}{\sqrt{\xi(y)^2 + \xi(w)^2}},$$

and the multiplicative reduced Sombor index (RSOII) [37],

$$RSOII(G) = \prod_{yw \in E_G} \sqrt{(\xi(y) - 1)^2 + (\xi(w) - 1)^2}.$$

In [38], the discriminative and predictive potential of a few Sombor indices were investigated. The study's findings demonstrate that these descriptors can be effectively used to simulate the thermodynamic characteristics of chemical substances.

In [39] is reported that there is a highly correlation between boiling points and Sombor indices of some chemical compounds such as benzenoid hydrocarbons. The authors showed that the index RSO can predict some chemical and physical properties including acentric Factors, SNar, HNar and Entropy. In [40], the chemical importance of the index SO was investigated and it was shown that this index has high accuracy for predicting physical properties compared to some established indices. In [41], the authors showed that the RSO has better predictive power compared to some known indices including the Forgotten index, the Randić index, and the Zagreb indices. Research exploring the chemical applications of these indices is presented in [39-48].

2. Materials and Methods

2.1 *Motivation*

Currently, one of the significant goals of medicine and pharmacology is successful cancer treatment. One of the types of cancer treatment is targeted therapy that targets proteins that control the division, growth and spread of cell cancer. With the improvements in pharmacology and nanotechnology, scientists are able to appreciate the basic biology of cancer and extend new treatments [49][50]. Targeted therapy with interfering specific proteins helps to decrease tumors' growth and spread in the body [51].

The HA plays a critical role in maintaining the stability of tissue. On the other hand, HA has the features such as non-toxic, biodegradable, non-immunogenic, and chemically modifiable. Therefore, it attracts remarkable interest from researchers for applications in biomedical science such as drug delivery approaches [2][52].

Delivery carriers of HA-based drugs enable several advantages such the stability of drugs in cancer treatment in physiological conditions, solving drawbacks of anticancer drugs, and chemically modifying for obtaining HA conjugates through functional groups [3].

One of the most well-known drugs in cancer treatment is PTX [53]. Because of several limitations of PTX such as poor solubility in water and lack of activity against drug-resistant cell lines, HA-PTX conjugates can improve these problems. In [54], the authors developed HA-based paclitaxel prodrug micelles to effectively target and treat human breast cancer. In [55], the authors developed the HA conjugated with paclitaxel to improve anticancer activity. Therefore, HA-PTX conjugates play an important role in the protection of the injured area against microorganisms.

HA-Curcumin conjugates are considered an effective therapeutic approach to optimize tissue distribution and improve clinical outcomes. HA-Curcumin conjugates are considered an effective therapeutic approach for optimizing tissue dispersion. Also, HA-Curcumin conjugates target tumor metastases in the treatment of many types of cancer [6]. Therefore, HA conjugated with curcumin is considered a pharmaceutical strategy to improve solubility in water, tissue distribution, and the promising outcomes of cancer treatment [56].

Computing the topological indices for drugs can provide a theoretical basis for a better understanding of their biological and physical properties that led to the preparation of new drugs [57].

2.2 *Molecular structure analysis of Hyaluronic Acid conjugates*

In this section, we study the molecular graphs of HA conjugated with paclitaxel and curcumin. To do this, we consider the molecular graphs $(HA-PTX)_n$ and $(HA-CC)_n$ of HA-paclitaxel conjugate and HA-curcumin conjugate, respectively, with n units' linear iteration. We obtain some topological degree-based indices including SO, MSO, RSO, $SOII$, $RSOII$, and $MSOII$. We used Matlab software for validation and plotting the mathematical results. We also used the Mathematica software for mathematical calculations.

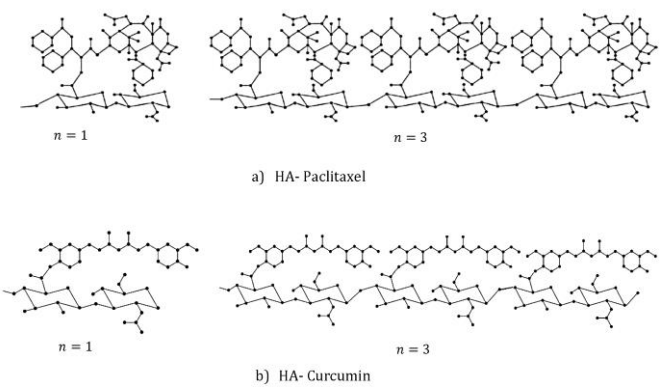

Figure 2
The molecular graphs of HA-conjugates when $n = 1$ and $n = 3$.

First, we consider the molecular graph $(HA-PTX)_n$ which is shown in Figure 2(a) for $n=1,3$. From the graph structure of $(HA-PTX)_n$, $|V|=87n+1$ and $|E|=96n$. For computing Sombor indices, we use the edge-partition approach for classifying edges of the molecular graph $(HA-PTX)_n$. The edge set of the graph $(HA-PTX)_n$ is divided as

$$E_{11}=\{yw\in E_G,\xi(y)=1,\xi(w)=1\},\quad E_{12}=\{yw\in E_G,\xi(y)=1,\xi(w)=2\},$$
$$E_{13}=\{yw\in E_G,\xi(y)=1,\xi(w)=3\},\quad E_{14}=\{yw\in E_G,\xi(y)=1,\xi(w)=4\},$$
$$E_{22}=\{yw\in E_G,\xi(y)=2,\xi(w)=2\},\quad E_{23}=\{yw\in E_G,\xi(y)=2,\xi(w)=3\},$$
$$E_{24}=\{yw\in E_G,\xi(y)=2,\xi(w)=4\},\quad E_{33}=\{yw\in E_G,\xi(y)=3,\xi(w)=3\},$$
$$E_{34}=\{yw\in E_G,\xi(y)=3,\xi(w)=4\},\quad E_{44}=\{yw\in E_G,\xi(y)=4,\xi(w)=4\}.$$

The number of edges in E_{ij}'s is shown in Table 1 and clearly, $|E_G|=\sum_{1\le i,j\le 4}|E_{ij}|$.

Table 1
The number of edges in subsets E_{ij}'s of $(HA-PTX)_n$.

E_{ij}	E_{11}	E_{12}	E_{13}	E_{14}	E_{22}	E_{23}	E_{24}	E_{33}	E_{34}	E_{44}
$\lvert E_{ij}\rvert$	0	$n+1$	$16n$	$4n$	$13n+1$	$32n-1$	$3n$	$19n-1$	$7n$	n

First, we investigate the graph $(HA-PTX)_n$ for computing some Sombor-type indices that are stated in this study.

Theorem 1: *For the molecular graph* $(HA-PTX)_n$,

i) $SO((HA-PTX)_n)=\left(87\sqrt{2}+7\sqrt{5}+16\sqrt{10}+32\sqrt{13}+4\sqrt{17}+35\right)n-\left(\sqrt{2}+\sqrt{13}-\sqrt{5}\right)$,

ii) $RSO((HA-PTX)_n)=\left(54\sqrt{2}+32\sqrt{5}+3\sqrt{10}+7\sqrt{13}+45\right)n-\left(\sqrt{2}+\sqrt{5}-1\right)$,

iii) $MSO((HA-PTX)_n)=\left(\frac{16}{\sqrt{10}}+\frac{32}{\sqrt{13}}+\frac{4}{\sqrt{17}}+\frac{157}{24}\sqrt{2}+\frac{\sqrt{5}}{2}+\frac{7}{5}\right)n+\left(\frac{1}{6\sqrt{2}}+\frac{1}{\sqrt{5}}-\frac{1}{\sqrt{13}}\right)$,

iv) $ASO((HA-PTX)_n)=\sqrt{2}(13n+1)\sqrt{\frac{(1-9n)^2}{(1+87n)^2}}+3\sqrt{2}(19n-1)\sqrt{\frac{(1+23n)^2}{(1+87n)^2}}+4\sqrt{2}n\sqrt{\frac{(1+39n)^2}{(1+87n)^2}}$

$$+(32n-1)\sqrt{\frac{13+342n+5085n^2}{(1+87n)^2}}+6n\sqrt{\frac{5+294n+6165n^2}{(1+87n)^2}}+16\sqrt{2}n\sqrt{\frac{5+102n+7893n^2}{(1+87n)^2}}$$
$$+(n+1)\sqrt{\frac{5-282n+11349n^2}{(1+87n)^2}}+7n\sqrt{\frac{25+1662n+29097n^2}{(1+87n)^2}}+4n\sqrt{\frac{17+1038n+35361n^2}{(1+87n)^2}},$$

for $n \geq 1$.

Proof: Suppose that G is the molecular graph $(HA-PTX)_n$ with $|V| = 87n + 1$ and $|E| = 96n$. According to Table 1, we obtain

i) $$\begin{aligned} SO(G) &= \sum_{yw\in E_G}\sqrt{\xi(y)^2+\xi(w)^2} \\ &= \sum_{yw\in E_{12}}\sqrt{5}+\sum_{yw\in E_{13}}\sqrt{10}+\sum_{yw\in E_{14}}\sqrt{17}+\sum_{yw\in E_{22}}\sqrt{8} \\ &\quad+\sum_{yw\in E_{23}}\sqrt{13}+\sum_{yw\in E_{24}}\sqrt{20}+\sum_{yw\in E_{33}}\sqrt{18} \\ &\quad+\sum_{yw\in E_{34}}\sqrt{25}+\sum_{yw\in E_{44}}\sqrt{32} \\ &= \sqrt{5}(n+1)+\sqrt{10}(16n)+4\sqrt{17}n+2\sqrt{2}(13n+1) \\ &\quad+\sqrt{13}(32n-1)+6n\sqrt{5}+3\sqrt{2}(19n-1)+35n+4\sqrt{2}n \\ &= \left(87\sqrt{2}+7\sqrt{5}+16\sqrt{10}+32\sqrt{13}+4\sqrt{17}+35\right)n \\ &\quad-\left(\sqrt{2}+\sqrt{13}-\sqrt{5}\right). \end{aligned}$$

ii) $$\begin{aligned} RSO(G) &= \sum_{yw\in E_G}\sqrt{(\xi(y)-1)^2+(\xi(w)-1)^2} \\ &= \sum_{yw\in E_{12}}\sqrt{1}+\sum_{yw\in E_{13}}\sqrt{4}+\sum_{yw\in E_{14}}\sqrt{9}+\sum_{yw\in E_{22}}\sqrt{2} \\ &\quad+\sum_{yw\in E_{23}}\sqrt{5}+\sum_{yw\in E_{24}}\sqrt{10}+\sum_{yw\in E_{33}}\sqrt{8}+\sum_{yw\in E_{34}}\sqrt{13} \\ &\quad+\sum_{yw\in E_{44}}\sqrt{18} \\ &= (n+1)+32n+12n+\sqrt{2}(13n+1)+\sqrt{5}(32n-1) \\ &\quad+3\sqrt{10}n+2\sqrt{2}(19n-1)\ +7n\sqrt{13}+6\sqrt{2}n \\ &= \left(54\sqrt{2}+32\sqrt{5}+3\sqrt{10}+7\sqrt{13}+45\right)n \\ &\quad-\left(\sqrt{2}+\sqrt{5}-1\right). \end{aligned}$$

iii) $$\begin{aligned} MSO(G) &= \sum_{yw\in E_G}\frac{1}{\sqrt{\xi(y)^2+\xi(w)^2}} \\ &= \sum_{yw\in E_{12}}\frac{1}{\sqrt{5}}+\sum_{yw\in E_{13}}\frac{1}{\sqrt{10}}+\sum_{yw\in E_{14}}\frac{1}{\sqrt{17}}+\sum_{yw\in E_{22}}\frac{1}{\sqrt{8}} \\ &\quad+\sum_{yw\in E_{23}}\frac{1}{\sqrt{13}}+\sum_{yw\in E_{24}}\frac{1}{\sqrt{20}}+\sum_{yw\in E_{33}}\frac{1}{\sqrt{18}} \\ &\quad+\sum_{yw\in E_{34}}\frac{1}{\sqrt{25}}+\sum_{yw\in E_{44}}\frac{1}{\sqrt{32}} \\ &= \frac{1}{\sqrt{5}}(n+1)+\frac{1}{\sqrt{10}}(16n)+\frac{4}{\sqrt{17}}n+\frac{1}{2\sqrt{2}}(13n+1) \\ &\quad+\frac{1}{\sqrt{13}}(32n-1)+\frac{3n}{2\sqrt{5}}+\frac{1}{3\sqrt{2}}(19n-1)+\frac{7n}{5}+\frac{1}{4\sqrt{2}}n \\ &= \left(\frac{16}{\sqrt{10}}+\frac{32}{\sqrt{13}}+\frac{4}{\sqrt{17}}+\frac{157}{24}\sqrt{2}+\frac{\sqrt{5}}{2}+\frac{7}{5}\right)n+\left(\frac{1}{6\sqrt{2}}+\frac{1}{\sqrt{5}}-\frac{1}{\sqrt{13}}\right). \end{aligned}$$

iv) Since $|V_G| = 87n + 1$ and $|E_G| = 96n$, we have

$$\begin{aligned}
ASO(G) &= \sum_{yw\in E_G}\sqrt{\left(\xi(y)-\frac{2|E_G|}{|V_G|}\right)^2+\left(\xi(w)-\frac{2|E_G|}{|V_G|}\right)^2}\\
&= (n+1)\sqrt{\left(1-\frac{192n}{1+87n}\right)^2+\left(2-\frac{192n}{1+87n}\right)^2}\\
&\quad +16n\sqrt{\left(1-\frac{192n}{1+87n}\right)^2+\left(3-\frac{192n}{1+87n}\right)^2}\\
&\quad +4n\sqrt{\left(1-\frac{192n}{1+87n}\right)^2+\left(4-\frac{192n}{1+87n}\right)^2}\\
&\quad +(13n+1)\sqrt{\left(2-\frac{192n}{1+87n}\right)^2+\left(2-\frac{192n}{1+87n}\right)^2}\\
&\quad +(32n-1)\sqrt{\left(2-\frac{192n}{1+87n}\right)^2+\left(3-\frac{192n}{1+87n}\right)^2}\\
&\quad +3n\sqrt{\left(2-\frac{192n}{1+87n}\right)^2+\left(4-\frac{192n}{1+87n}\right)^2}\\
&\quad +(19n-1)\sqrt{\left(3-\frac{192n}{1+87n}\right)^2+\left(3-\frac{192n}{1+87n}\right)^2}\\
&\quad +7n\sqrt{\left(3-\frac{192n}{1+87n}\right)^2+\left(4-\frac{192n}{1+87n}\right)^2}\\
&\quad +n\sqrt{\left(4-\frac{192n}{1+87n}\right)^2+\left(4-\frac{192n}{1+87n}\right)^2}\\
&= \sqrt{2}(13n+1)\sqrt{\frac{(1-9n)^2}{(1+87n)^2}}+3\sqrt{2}(19n-1)\sqrt{\frac{(1+23n)^2}{(1+87n)^2}}\\
&\quad +4\sqrt{2}n\sqrt{\frac{(1+39n)^2}{(1+87n)^2}}+(32n-1)\sqrt{\frac{13+342n+5085n^2}{(1+87n)^2}}\\
&\quad +6n\sqrt{\frac{5+294n+6165n^2}{(1+87n)^2}}+16\sqrt{2}n\sqrt{\frac{5+102n+7893n^2}{(1+87n)^2}}\\
&\quad +(n+1)\sqrt{\frac{5-282n+11349n^2}{(1+87n)^2}}+7n\sqrt{\frac{25+1662n+29097n^2}{(1+87n)^2}}\\
&\quad +4n\sqrt{\frac{17+1038n+35361n^2}{(1+87n)^2}}.
\end{aligned}$$

In the next theorem, we compute the multiplicative Sombor-type indices of the molecular graph $(HA-PTX)_n$ that are stated in this study.

Theorem 2: For the molecular graph $(HA-PTX)_n$,

i) $SOII((HA-PTX)_n) = \left(\sqrt{2}\right)^{85n+2} \times \left(\sqrt{5}\right)^{34n+1} \times \left(\sqrt{13}\right)^{32n-1} \times 3^{19n-1} \times 289^n$,

ii) $RSOII((HA-PTX)_n) = \left(\sqrt{5}\right)^{35n-1} \times \left(\sqrt{13}\right)^{7n} \times 2^{53n-1} \times 243^n$,

iii) $MSOII((HA-PTX)_n) = \left(\frac{1}{\sqrt{2}}\right)^{49n} \times \left(\frac{1}{2}\right)^{18n+1} \times \left(\frac{1}{3}\right)^{19n-1} \times \left(\frac{1}{5}\right)^{17n} \times \left(\frac{1}{17}\right)^{2n}$,

for $n \geq 1$.

Proof: Suppose that G is the molecular graph $(HA-PTX)_n$. According to Table 1 and the definition of the multiplicative Sombor indices, we get

i) $$\begin{aligned} SOII(G) &= \prod_{yw\in E_G} \sqrt{\xi(y)^2+\xi(w)^2} \\ &= \prod_{yw\in E_{12}} \sqrt{5} \times \prod_{yw\in E_{13}} \sqrt{10} \times \prod_{yw\in E_{14}} \sqrt{17} \times \prod_{yw\in E_{22}} \sqrt{8} \\ &\quad \times \prod_{yw\in E_{23}} \sqrt{13} \times \prod_{yw\in E_{24}} \sqrt{20} \times \prod_{yw\in E_{33}} \sqrt{18} \\ &\quad \times \prod_{yw\in E_{34}} \sqrt{25} \times \prod_{yw\in E_{44}} \sqrt{32} \\ &= \left(\sqrt{5}\right)^{n+1} \times \left(\sqrt{5}\right)^{16n} \times \left(\sqrt{17}\right)^{4n} \times \left(\sqrt{8}\right)^{13n+1} \times \left(\sqrt{13}\right)^{32n-1} \\ &\quad \times \left(\sqrt{20}\right)^{3n} \times \left(\sqrt{18}\right)^{19n-1} \times \left(\sqrt{25}\right)^{7n} \times \left(\sqrt{32}\right)^{n} \\ &= \left(\sqrt{5}\right)^{n+1} \times \left(\sqrt{5}\right)^{16n} \times (17)^{2n} \times \left(2\sqrt{2}\right)^{13n+1} \times \left(\sqrt{13}\right)^{32n-1} \\ &\quad \times \left(2\sqrt{5}\right)^{3n} \times \left(3\sqrt{2}\right)^{19n-1} \times (5)^{7n} \times \left(4\sqrt{2}\right)^{n} \\ &= \left(\sqrt{2}\right)^{85n+2} \times \left(\sqrt{5}\right)^{34n+1} \times \left(\sqrt{13}\right)^{32n-1} \times 3^{19n-1} \times 289^{n}. \end{aligned}$$

ii) $$\begin{aligned} RSOII(G) &= \prod_{yw\in E_G} \sqrt{(\xi(y)-1)^2+(\xi(w)-1)^2} \\ &= \prod_{yw\in E_{12}} \sqrt{1} \times \prod_{yw\in E_{13}} \sqrt{4} \times \prod_{yw\in E_{14}} \sqrt{9} \times \prod_{yw\in E_{22}} \sqrt{2} \\ &\quad \times \prod_{yw\in E_{23}} \sqrt{5} \times \prod_{yw\in E_{24}} \sqrt{10} \times \prod_{yw\in E_{33}} \sqrt{8} \\ &\quad \times \prod_{yw\in E_{34}} \sqrt{13} \times \prod_{yw\in E_{44}} \sqrt{18} \\ &= (2)^{16n} \times (3)^{4n} \times \left(\sqrt{2}\right)^{13n+1} \times \left(\sqrt{5}\right)^{32n-1} \times \left(\sqrt{10}\right)^{3n} \\ &\quad \times \left(\sqrt{8}\right)^{19n-1} \times \left(\sqrt{13}\right)^{7n} \times \left(\sqrt{18}\right)^{n} \\ &= \left(\sqrt{5}\right)^{35n-1} \times \left(\sqrt{13}\right)^{7n} \times 2^{53n-1} \times 243^{n}. \end{aligned}$$

iii) $$\begin{aligned} MSOII(G) &= \prod_{yw\in E_G} \frac{1}{\sqrt{\xi(y)^2+\xi(w)^2}} \\ &= \prod_{yw\in E_{12}} \frac{1}{\sqrt{5}} \times \prod_{yw\in E_{13}} \frac{1}{\sqrt{10}} \times \prod_{yw\in E_{14}} \frac{1}{\sqrt{17}} \times \prod_{yw\in E_{22}} \frac{1}{\sqrt{8}} \\ &\quad \times \prod_{yw\in E_{23}} \frac{1}{\sqrt{13}} \times \prod_{yw\in E_{24}} \frac{1}{\sqrt{20}} \times \prod_{yw\in E_{33}} \frac{1}{\sqrt{18}} \\ &\quad \times \prod_{yw\in E_{34}} \frac{1}{\sqrt{25}} \times \prod_{yw\in E_{44}} \frac{1}{\sqrt{32}} \\ &= \left(\frac{1}{\sqrt{5}}\right)^{n+1} \times \left(\frac{1}{\sqrt{10}}\right)^{16n} \times \left(\frac{1}{\sqrt{17}}\right)^{4n} \times \left(\frac{1}{2\sqrt{2}}\right)^{13n+1} \times \left(\frac{1}{\sqrt{13}}\right)^{32n-1} \\ &\quad \times \left(\frac{1}{2\sqrt{5}}\right)^{3n} \times \left(\frac{1}{3\sqrt{2}}\right)^{19n-1} \times \left(\frac{1}{5}\right)^{7n} \times \left(\frac{1}{4\sqrt{2}}\right)^{n} \\ &= \left(\frac{1}{\sqrt{2}}\right)^{49n} \times \left(\frac{1}{2}\right)^{18n+1} \times \left(\frac{1}{3}\right)^{19n-1} \times \left(\frac{1}{5}\right)^{17n} \times \left(\frac{1}{17}\right)^{2n}. \end{aligned}$$

Next, we study the molecular graph $(HA-CC)_n$ of HA-curcumin conjugate which is shown in Figure 2(b) for $n=1,3$. From the graph structure of $(HA-CC)_n$, we have $|V_G|=52n+1$ and $|E_G|=56n$. According to the edge-partition method, for graph $(HA-PTX)_n$ we have

$$E_{11}=\{yw\in E_G,\xi(y)=1,\xi(w)=1\},$$
$$E_{12}=\{yw\in E_G,\xi(y)=1,\xi(w)=2\},$$
$$E_{13}=\{yw\in E_G,\xi(y)=1,\xi(w)=3\},$$
$$E_{22}=\{yw\in E_G,\xi(y)=2,\xi(w)=2\},$$
$$E_{23}=\{yw\in E_G,\xi(y)=2,\xi(w)=3\},$$
$$E_{33}=\{yw\in E_G,\xi(y)=3,\xi(w)=3\}.$$

The number of edges in E_{ij}'s is shown in Table 2 and we have $|E_G|=\sum_{1\le i,j\le 3}|E_{ij}|$.

Table 2
The number of edges in subsets E_{ij}'s of $(HA-CC)_n$.

E_{ij}	E_{11}	E_{12}	E_{13}	E_{22}	E_{23}	E_{33}
$\lvert E_{ij}\rvert$	0	$3n+1$	$9n$	$4n+1$	$29n-1$	$11n-1$

Theorem 3: *For the molecular graph $(HA-CC)_n$ with n units' linear iteration, we have*

i) $SO((HA-CC)_n)=\left(41\sqrt{2}+3\sqrt{5}+9\sqrt{10}+29\sqrt{13}\right)n-\left(\sqrt{2}-\sqrt{5}+\sqrt{13}\right)$,

ii) $RSO((HA-CC)_n)=\left(26\sqrt{2}+29\sqrt{5}+21\right)n-(\sqrt{2}+\sqrt{5}-1)$,

iii) $MSO((HA-CC)_n)=\left(\frac{17}{3\sqrt{2}}+\frac{3}{\sqrt{5}}+\frac{9}{\sqrt{10}}+\frac{29}{\sqrt{13}}\right)n+\left(\frac{1}{6\sqrt{2}}+\frac{1}{\sqrt{5}}-\frac{1}{\sqrt{13}}\right)$,

iv) $ASO((HA-CC)_n)=2\sqrt{2}(4n+1)\sqrt{\frac{(1-4n)^2}{(1+52n)^2}}+\sqrt{2}(11n-1)\sqrt{\frac{(3+44n)^2}{(1+52n)^2}}$
$+(29n-1)\sqrt{\frac{13+232n+2000n^2}{(1+52n)^2}}+9\sqrt{2}n\sqrt{\frac{5+72n+2768n^2}{(1+52n)^2}}$
$+(3n+1)\sqrt{\frac{5-152n+3664n^2}{(1+52n)^2}}$,

for $n\ge 1$.

Proof: Suppose that G is the molecular graph $(HA-CC)_n$ with $|V_G|=52n+1$ and $|E_G|=56n$. According to Table 2, we get

i) $SO(G)=\sum_{uv\in E}\sqrt{\xi(y)^2+\xi(w)^2}$
$=\sum_{yw\in E_{12}}\sqrt{5}+\sum_{yw\in E_{13}}\sqrt{10}+\sum_{yw\in E_{22}}\sqrt{8}+\sum_{yw\in E_{23}}\sqrt{13}$
$+\sum_{yw\in E_{33}}\sqrt{18}$

$$= \sqrt{5}(3n+1) + \sqrt{10}(9n) + \sqrt{8}(4n+1) + \sqrt{13}(29n-1) + \sqrt{18}(11n-1)$$
$$= \left(41\sqrt{2} + 3\sqrt{5} + 9\sqrt{10} + 29\sqrt{13}\right)n - \left(\sqrt{2} - \sqrt{5} + \sqrt{13}\right).$$

ii) $RSO(G) = \sum_{yw \in E_G} \sqrt{(\xi(y)-1)^2 + (\xi(w)-1)^2}$
$$= \sum_{yw \in E_{12}} \sqrt{1} + \sum_{yw \in E_{13}} \sqrt{4} + \sum_{yw \in E_{22}} \sqrt{2} + \sum_{yw \in E_{23}} \sqrt{5} + \sum_{yw \in E_{33}} \sqrt{8}$$
$$= (3n+1) + 18n + \sqrt{2}(4n+1) + \sqrt{5}(29n-1) + 2\sqrt{2}(11n-1)$$
$$= \left(26\sqrt{2} + 29\sqrt{5} + 21\right)n - \left(\sqrt{2} + \sqrt{5} - 1\right).$$

iii) $MSO(G) = \sum_{yw \in E_G} \frac{1}{\sqrt{\xi(y)^2 + \xi(w)^2}}$
$$= \sum_{yw \in E_{12}} \frac{1}{\sqrt{5}} + \sum_{yw \in E_{13}} \frac{1}{\sqrt{10}} + \sum_{yw \in E_{22}} \frac{1}{\sqrt{8}} + \sum_{yw \in E_{23}} \frac{1}{\sqrt{13}} + \sum_{yw \in E_{33}} \frac{1}{\sqrt{18}}$$
$$= \frac{1}{\sqrt{5}}(3n+1) + \frac{1}{\sqrt{10}}(9n) + \frac{1}{2\sqrt{2}}(4n+1) + \frac{1}{\sqrt{13}}(29n-1) + \frac{1}{3\sqrt{2}}(11n-1)$$
$$= \left(\frac{17}{3\sqrt{2}} + \frac{3}{\sqrt{5}} + \frac{9}{\sqrt{10}} + \frac{29}{\sqrt{13}}\right)n + \left(\frac{1}{6\sqrt{2}} + \frac{1}{\sqrt{5}} - \frac{1}{\sqrt{13}}\right).$$

iv) $ASO(G) = \sum_{yw \in E_G} \sqrt{\left(\xi(y) - \frac{2|E_G|}{|V_G|}\right)^2 + \left(\xi(w) - \frac{2|E_G|}{|V_G|}\right)^2}$
$$= (3n+1)\sqrt{\left(1 - \frac{112n}{52n+1}\right)^2 + \left(2 - \frac{112n}{52n+1}\right)^2} + 9n\sqrt{\left(1 - \frac{112n}{52n+1}\right)^2 + \left(3 - \frac{112n}{52n+1}\right)^2} + (4n+1)\sqrt{\left(2 - \frac{112n}{52n+1}\right)^2 + \left(2 - \frac{112n}{52n+1}\right)^2} + (29n-1)\sqrt{\left(2 - \frac{112n}{52n+1}\right)^2 + \left(3 - \frac{112n}{52n+1}\right)^2} + (11n-1)\sqrt{\left(3 - \frac{112n}{52n+1}\right)^2 + \left(3 - \frac{112n}{52n+1}\right)^2}$$
$$= 2\sqrt{2}(4n+1)\sqrt{\frac{(1-4n)^2}{(1+52n)^2}} + \sqrt{2}(11n-1)\sqrt{\frac{(3+44n)^2}{(1+52n)^2}} + (29n-1)\sqrt{\frac{13+232n+2000n^2}{(1+52n)^2}} + 9\sqrt{2}n\sqrt{\frac{5+72n+2768n^2}{(1+52n)^2}} + (3n+1)\sqrt{\frac{5-152n+3664n^2}{(1+52n)^2}}.$$

Theorem 4: *For the molecular graph* $(HA-CC)_n$ *with* n *units' linear iteration, we have*

i) $SOII((HA-CC)_n) = \left(\sqrt{5}\right)^{12n+1} \times \left(\sqrt{13}\right)^{29n-1} \times 2^{16n+1} \times 3^{11n-1}$,

ii) $RSOII((HA-CC)_n) = \left(\sqrt{2}\right)^{15n} \times \left(\sqrt{5}\right)^{29n-1} \times 2^{20n-1}$,

iii) $MSOII((HA-CC)_n) = \left(\frac{1}{\sqrt{5}}\right)^{12n+1} \times \left(\frac{1}{\sqrt{13}}\right)^{29n-1} \times \left(\frac{1}{2}\right)^{16n+1} \times \left(\frac{1}{3}\right)^{11n-1}$,

for $n \geq 1$.

Proof: Suppose that G is the molecular graph $(HA-CC)_n$. According to Table 2, we have

i) $$\begin{aligned} SOII(G) &= \prod_{yw\in E_G} \sqrt{\xi(y)^2+\xi(w)^2} \\ &= \prod_{yw\in E_{12}} \sqrt{5} \times \prod_{yw\in E_{13}} \sqrt{10} \times \prod_{yw\in E_{22}} \sqrt{8} \times \prod_{yw\in E_{23}} \sqrt{13} \\ &\quad \times \prod_{yw\in E_{33}} \sqrt{18} \\ &= \left(\sqrt{5}\right)^{3n+1} \times \left(\sqrt{10}\right)^{9n} \times \left(\sqrt{8}\right)^{4n+1} \times \left(\sqrt{13}\right)^{29n-1} \\ &\quad \times \left(\sqrt{18}\right)^{11n-1} \\ &= \left(\sqrt{5}\right)^{12n+1} \times \left(\sqrt{13}\right)^{29n-1} \times 2^{16n+1} \times 3^{11n-1}. \end{aligned}$$

ii) $$\begin{aligned} RSOII(G) &= \prod_{yw\in E_G} \sqrt{(\xi(y)-1)^2+(\xi(w)-1)^2} \\ &= \prod_{yw\in E_{12}} \sqrt{1} \times \prod_{yw\in E_{13}} \sqrt{4} \times \prod_{yw\in E_{22}} \sqrt{2} \times \prod_{yw\in E_{23}} \sqrt{5} \\ &\quad \times \prod_{yw\in E_{33}} \sqrt{8} \\ &= 2^{9n} \times \left(\sqrt{2}\right)^{4n+1} \times \left(\sqrt{5}\right)^{29n-1} \times \left(2\sqrt{2}\right)^{11n-1} \\ &= \left(\sqrt{2}\right)^{15n} \times \left(\sqrt{5}\right)^{29n-1} \times 2^{20n-1}. \end{aligned}$$

iii) $$\begin{aligned} MSOII(G) &= \prod_{yw\in E_G} \frac{1}{\sqrt{\xi(y)^2+\xi(w)^2}} \\ &= \prod_{yw\in E_{12}} \frac{1}{\sqrt{5}} \times \prod_{yw\in E_{13}} \frac{1}{\sqrt{10}} \times \prod_{yw\in E_{22}} \frac{1}{\sqrt{8}} \times \prod_{yw\in E_{23}} \frac{1}{\sqrt{13}} \\ &\quad \times \prod_{yw\in E_{33}} \frac{1}{\sqrt{18}} \\ &= \left(\frac{1}{\sqrt{5}}\right)^{3n+1} \times \left(\frac{1}{\sqrt{10}}\right)^{9n} \times \left(\frac{1}{2\sqrt{2}}\right)^{4n+1} \times \left(\frac{1}{\sqrt{13}}\right)^{29n-1} \times \left(\frac{1}{3\sqrt{2}}\right)^{11n-1} \\ &= \left(\frac{1}{\sqrt{5}}\right)^{12n+1} \times \left(\frac{1}{\sqrt{13}}\right)^{29n-1} \times \left(\frac{1}{2}\right)^{16n+1} \times \left(\frac{1}{3}\right)^{11n-1}. \end{aligned}$$

3. Results and discussions

Calculating topological indices of drug structure enables researchers to better understand the biological, physicochemical properties of drugs. Hence, we studied the structures of HA-PTX/Curcumin conjugates and obtained some Sombor indices and the multiplicative Sombor indices.

Tables 5-8 show the numerical outcomes of the topological indices studied of HA-Paclitaxel and HA-Curcumin. Also, the graphical comparison of the results for the indices of SO, RSO, ASO, and MSO is shown in Figures 3 and 4.

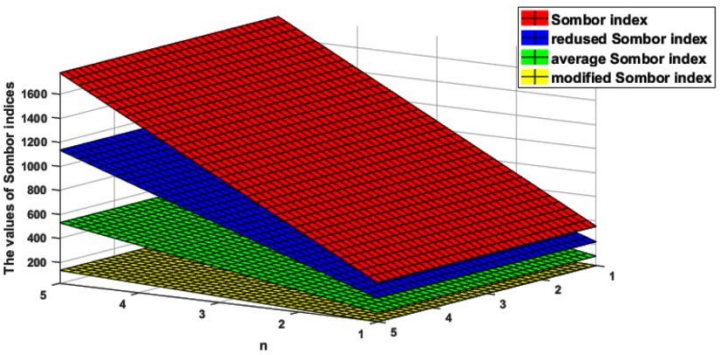

Figure 3
Comparison of SO, RSO, ASO, and MSO for the HA-Paclitaxel structure.

It can be observed from Figures 3 and 4, that SO (with red color), RSO (with blue color), MSO (with green color), and ASO (with yellow color) for the HA-PTX and HA-Curcumin increase with the increase in n. According to the results in Theorems 1 and 3, the linear functions of these four Sombor indices of the molecular graphs HA-Paclitaxel and HA-Curcumin are obtained. Based on Tables 3 and 4, the following relations of SO, RSO, MSO, and ASO functions for $(HA-PTX)_n$ and $(HA-CC)_n$ are obtained.

For any $n \geq 1$,

$$MSO((HA-PTX)_n) \leq ASO((HA-PTX)_n) \leq RSO((HA-PTX)_n) \leq SO((HA-PTX)_n),$$

and

$$MSO((HA-CC)_n) \leq ASO((HA-CC)_n) \leq RSO((HA-CC)_n) \leq SO((HA-CC)_n).$$

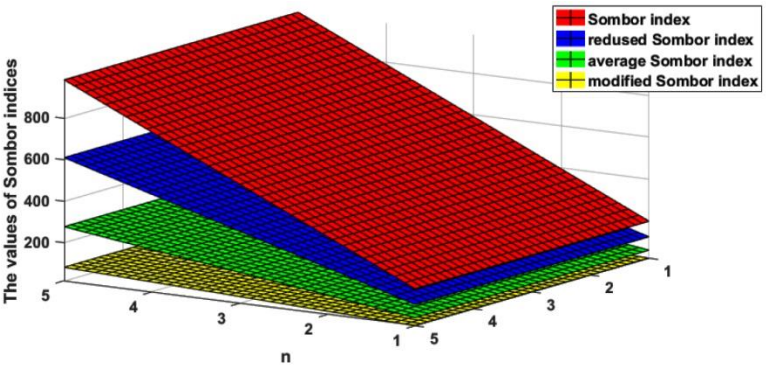

Figure 4
Comparison of SO, RSO, ASO, and MSO for the HA-Curcumin structure.

Table 3
The results obtained for SO, RSO, ASO, and MSO of the molecular graph HA-Paclitaxel.

Sombor indices	The exact values in terms of n	Function
$SO((HA-PTX)_n)$	$\left(41\sqrt{2}+3\sqrt{5}+9\sqrt{10}+29\sqrt{13}\right)n - \left(\sqrt{2}-\sqrt{5}+\sqrt{13}\right)$	$\approx 356.156n - 2.7837$
$RSO((HA-PTX)_n)$	$\left(26\sqrt{2}+29\sqrt{5}+21\right)n-(\sqrt{2}+\sqrt{5}-1)$	$\approx 227.647n - 2.6503$
$MSO((HA-PTX)_n)$	$\left(\frac{16}{\sqrt{10}}+\frac{157}{24}\sqrt{2}+\frac{\sqrt{5}}{2}+\frac{32}{\sqrt{13}}+\frac{4}{\sqrt{17}}+\frac{7}{5}\right)n + \left(\frac{1}{6\sqrt{2}}+\frac{1}{\sqrt{5}}-\frac{1}{\sqrt{13}}\right)$	$\approx 26.6743n - 0.2877$
$ASO((HA-PTX)_n)$	$\sqrt{2}(13n+1)\sqrt{\frac{(1-9n)^2}{(1+87n)^2}}+3\sqrt{2}(19n-1)\sqrt{\frac{(1+23n)^2}{(1+87n)^2}}+4\sqrt{2}n\sqrt{\frac{(1+39n)^2}{(1+87n)^2}}+(32n-1)\sqrt{\frac{13+342n+5085n^2}{(1+87n)^2}}+6n\sqrt{\frac{5+294n+6165n^2}{(1+87n)^2}}+16\sqrt{2}n\sqrt{\frac{5+102n+7893n^2}{(1+87n)^2}}+(n+1)\sqrt{\frac{5-282n+11349n^2}{(1+87n)^2}}+7n\sqrt{\frac{25+1662n+29097n^2}{(1+87n)^2}}+4n\sqrt{\frac{17+1038n+35361n^2}{(1+87n)^2}}$,	$\approx 105.996n - 0.4242$

Table 4
The results obtained for SO, RSO, ASO, and MSO of the molecular graph HA-Curcumin.

Sombor indices	The exact values in terms of n	Function
$SO((HA-CC)_n)$	$\left(87\sqrt{2}+7\sqrt{5}+16\sqrt{10}+32\sqrt{13}+4\sqrt{17}+35\right)n-\left(\sqrt{2}+\sqrt{13}-\sqrt{5}\right)$	$\approx 197.712n - 2.7837$
$RSO((HA-CC)_n)$	$\left(54\sqrt{2}+32\sqrt{5}+3\sqrt{10}+7\sqrt{13}+45\right)n-\left(\sqrt{2}+\sqrt{5}-1\right)$	$\approx 122.616n - 2.6503$
$MSO((HA-CC)_n)$	$\left(\frac{17}{3\sqrt{2}}+\frac{3}{\sqrt{5}}+\frac{9}{\sqrt{10}}+\frac{29}{\sqrt{13}}\right)n+\left(\frac{1}{6\sqrt{2}}+\frac{1}{\sqrt{5}}-\frac{1}{\sqrt{13}}\right)$	$\approx 16.2378n + 0.2877$
$ASO((HA-CC)_n)$	$2\sqrt{2}(4n+1)\sqrt{\frac{(1-4n)^2}{(1+52n)^2}}+\sqrt{2}(11n-1)\sqrt{\frac{(3+44n)^2}{(1+52n)^2}}+(29n-1)\sqrt{\frac{13+232n+2000n^2}{(1+52n)^2}}+9\sqrt{2}n\sqrt{\frac{5+72n+2768n^2}{(1+52n)^2}}+(3n+1)\sqrt{\frac{5-152n+3664n^2}{(1+52n)^2}}$	$\approx 55.3439n - 0.675$

Based on Theorems 2 and 4, the multiplicative Sombor indices exhibit exponential growth. Tables 6 and 8 demonstrate this behavior, showing that the indices $SOII$ and $RSOII$ increase as the value of n increases. The function of $MSOII$ decreases in any two structures of HA-conjugates. Therefore, the functions of $SOII$ and $RSOII$ are increasing functions and the function $MSOII$ is the decreasing function for the molecular graphs $(HA-PTX)_n$ and $(HA-CC)_n$ (see Figures 5 and 6).

Table 5
Numerical results for SO, RSO, ASO, and MSO of HA-Paclitaxel.

$(HA-PTX)_n$	SO	RSO	ASO	MSO
$n=1$	353.3718	224.9971	106.4831	26.9620
$n=2$	709.5274	452.6445	212.5301	53.6363
$n=3$	1065.6829	680.2919	318.5429	80.3107
$n=4$	1421.8385	907.9393	424.5470	106.9850
$n=5$	1777.9941	1135.5867	530.5478	133.6594

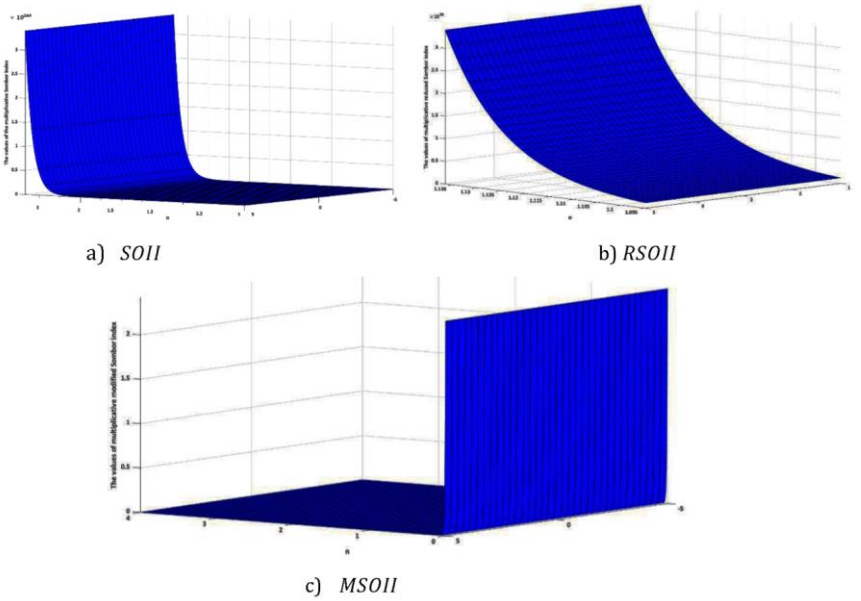

a) $SOII$ b) $RSOII$

c) $MSOII$

Figure 5
Charts of $SOII$, $RSOII$, and $MSOII$ for the HA-Paclitaxel structure.

Table 6
Numerical results related to of *SOII*, *RSOII*, and *MSOII* for the HA-Paclitaxel structure.

$(HA-PTX)_n$	$SOII$	$RSOII$	$MSOII$
$n=1$	4.38×10^{53}	6.61×10^{33}	2.28×10^{-54}
$n=2$	4.65×10^{107}	1.95×10^{68}	2.15×10^{-108}
$n=3$	4.93×10^{161}	5.78×10^{102}	2.02×10^{-162}
$n=4$	5.23×10^{215}	1.71×10^{137}	1.91×10^{-216}
$n=5$	5.54×10^{269}	5.06×10^{171}	1.80×10^{-270}

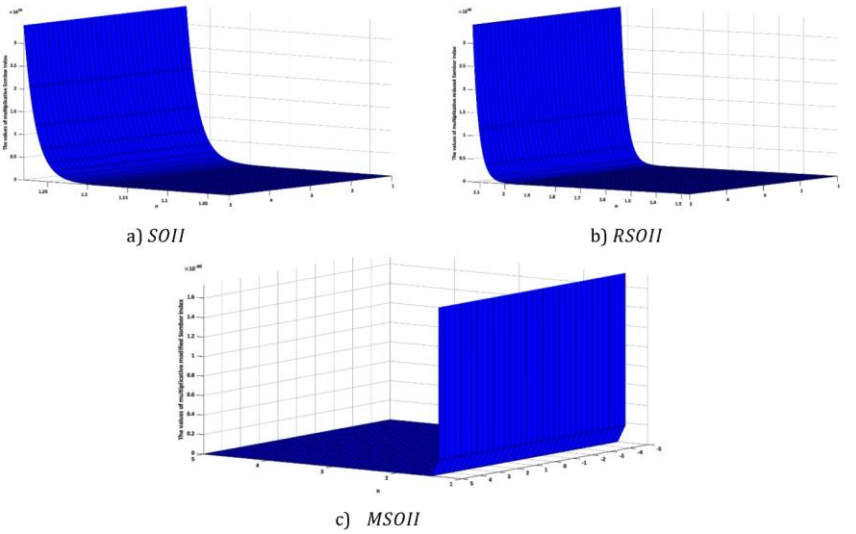

a) *SOII* b) *RSOII*

c) *MSOII*

Figure 6
Charts of *SOII*, *RSOII*, and *MSOII* for the HA-Curcumin structure.

Table 7
Numerical results related to *SO*, *RSO*, *ASO*, and *MSO* of the HA-Curcumin structure.

$(HA-CC)_n$	SO	RSO	ASO	MSO
$n=1$	194.9287	119.9652	55.6583	16.5254
$n=2$	392.6411	242.5807	111.0861	32.7632
$n=3$	590.3536	365.1962	166.4580	49.0010
$n=4$	788.0660	487.8118	221.8159	65.2388
$n=5$	985.7785	610.4273	277.1683	81.4766

Table 8
Numerical results related to $SOII$, $RSOII$, and $MSOII$ of the HA-Curcumin structure.

$(HA-CC)_n$	$SOII$	$RSOII$	$MSOII$
$n=1$	1.06×10^{30}	5.79×10^{17}	9.39×10^{-31}
$n=2$	2.74×10^{60}	1.50×10^{36}	3.64×10^{-61}
$n=3$	7.06×10^{90}	3.88×10^{54}	1.41×10^{-91}
$n=4$	1.81×10^{121}	1.007×10^{73}	5.49×10^{-122}
$n=5$	4.68×10^{151}	2.60×10^{91}	2.13×10^{-152}

4. Conclusion

Recent studies have shown that some Sombor indices are able to predict the physical and chemical properties of structures. In this work, some new topological indices of HA-PTX and HA-curcumin conjugates are computed by using the graph theory.

Tables 5-8 present the numerical outcomes of Sombor-type indices of the structures HA-Paclitaxel/Curcumin conjugates. These results can predict physical and chemical properties including Entropy, boiling points, molar volume, SNar, density, and HNar of HA–Paclitaxel/curcumin conjugates.

According to Figures 3-6 for the two molecular structures of HA-Paclitaxel and HA-Curcumin, the Sombor indices and the multiplicative Sombor indices increase with the increase in n except for the index $MSOII$ which decreases in any two structures of HA-conjugates.

The linear functions of Sombor indices of the molecular graphs HA-Paclitaxel and HA-Curcumin conjugated computed based on the results obtained in Theorems 1 and 3. These results are shown in Tables 3 and 4.

The results in this study can be used in applications of QSPR models including anticancer drug research. The computation of other Sombor indices of the molecular structure of anticancer drugs would be an interesting topic for further study.

References

[1] J. Drbohlavova, J. Chomoucka, V. Adam, M. Ryvolova, T. Eckschlager, J. Hubalek, and R. Keizek, "Nanocarriers for anticancer drug-new trends in nanomedicine," *Curr. Drug Metab.*, vol. 14, pp. 547–564 (2013), doi: 10.2174/1389200211314050005.

[2] L. Lapčík, L. Lapcik, S. De Smedt, J. Demeester, and P. Chabrecek, "Hyaluronan: Preparation, structure, properties, and applications," *Chem. Rev.*, vol. 98, pp. 2663–2684 (1998).

[3] T. C. Laurent and J. Fraser, "Hyaluronan," *FASEB J.*, vol. 6, pp. 2397–2404 (1992).

[4] A. Fallacara, E. Baldini, S. Manfredini, and S. Vertuani, "Hyaluronic acid in the third millennium," *Polymers* (Basel)., vol. 10, p. 701 (2018).

[5] S. Manju and K. Sreenivasan, "Conjugation of curcumin onto hyaluronic acid enhances its aqueous solubility and stability," *J. Colloid Interface Sci.*, vol. 359, no. 1, pp. 318–325 (2011).

[6] G. Saravanakumar, V. G. Deepagan, R. Jayakumar, and J. H. Park, "Hyaluronic acid-based conjugates for tumor-targeted drug delivery and imaging," *J. Biomed. Nanotechnol.*, vol. 10, pp. 17–31 (2014).

[7] H. Lee, K. Lee, and T. G. Park, "Hyaluronic acid-paclitaxel conjugate micelles: synthesis, characterization, and antitumor activity," *Bioconjug. Chem.*, vol. 19, no. 6, pp. 1319–1325 (2008).

[8] T. M. Mekhail and M. Markman, "Paclitaxel in cancer therapy," Expert Opin. *Pharmacother.*, vol. 3, pp. 755–766 (2002).

[9] D. Xin, Y. Wang, and J. Xiang, "The use of amino acid linkers in the conjugation of paclitaxel with hyaluronic acid as drug delivery system: Synthesis, self-assembled property, drug release, and in vitro efficiency," *Pharm. Res.*, vol. 27, pp. 380–389 (2010).

[10] B. B. Aggarwal, A. Kumar, and A. C. Bharti, "Anticancer potential of curcumin: Preclinical and clinical studies," *Anticancer Res.*, vol. 23, pp. 363–398 (2003).

[11] K. M. Nelson, J. L. Dahlin, J. Bisson, J. Graham, G. F. Pauli, and M. A. Walters, "The essential medicinal chemistry of curcumin," *J. Med. Chem.*, vol. 60, no. 5, pp. 1620–1637 (2017).

[12] M. Kharat and D. J. McClements, "Recent advances in colloidal delivery systems for nutraceuticals: A case study–Delivery by design of curcumin," *J. Colloid Interface Sci.*, vol. 557, pp. 506–518 (2019).

[13] D. Bonchev, Chemical Graph Theory: Introduction and Fundamentals, Abacus Press/Gordon & Breach, New York (1991).

[14] T. Hendrik, R. Todeschini, C. Viviana, M. Raimund, and K. Hugo, Handbook of Molecular Descriptors, Wiley-VCH, Weinheim (2002).

[15] J. C. Dearden, "The use of topological indices in QSAR and QSPR modeling," in Advances in QSAR Modeling, Springer, Berlin, Germany, pp. 57–88 (2017).

[16] A. Mauri, V. Consonni, and R. Todeschini, "Molecular descriptors," in Handbook of Computational Chemistry, J. Leszczynski, Ed. Springer Netherlands, Dordrecht, Netherlands, pp. 1–29 (2016).

[17] H. Wiener, "Structural determination of paraffin boiling points," *J. Am. Chem. Soc.,* vol. 69, no. 1, pp. 17–20 (1974).

[18] I. Gutman, E. Milovanovic, and I. Milovanovic, "Beyond the Zagreb indices," *AKCE Int. J. Graphs Combin.*, vol. 17, no. 1, pp. 74–85 (2018).

[19] M. Imran, A. Q. Baig, H. M. A. Siddiqui, and R. Sarwar, "On molecular topological properties of diamond-like networks," *Can. J. Chem.,* vol. 95, no. 7, pp. 758–770 (2017).

[20] A. Q. Baig, M. Imran, W. Khalid, and N. Naeem, "Molecular description of carbon graphite and crystal cubic carbon structures," *Can. J. Chem.*, vol. 95, no. 6, pp. 674–686 (2017).

[21] K. C. Das, I. Gutman, and B. Furtula, "Survey on geometric-arithmetic indices of graphs," *MATCH Commun. Math. Comput. Chem.,* vol. 65, no. 3, pp. 595–644 (2011).

[22] A. Ali, W. Nazeer, M. Munir, and S. M. Kang, "M-polynomials and topological indices of zigzag and rhombic benzenoid systems," *Open Chem.*, vol. 16, no. 1, pp. 73–78 (2018).

[23] F. Movahedi, M. H. Akhbari, and H. Kamarulhaili, "On the Hosoya index of some families of graph," *Math. Interdisc. Res.,* vol. 6, pp. 225–234 (2021).

[24] I. Gutman and K. C. Das, "The first Zagreb index 30 years after," *MATCH Commun. Math. Comput. Chem.,* vol. 50, no. 1, pp. 83–92 (2004).

[25] M. Riaz, W. Gao, and A. Q. Baig, "M-polynomials and degree-based topological indices of some families of convex polytopes," *Open J. Math. Sci.*, vol. 2, no. 1, pp. 18–28 (2018).

[26] F. Movahedi, "Matching polynomials for some nanostar dendrimers," *Asian-European J. Math.,* vol. 14, no. 10, p. 2150188 (2021).

[27] A. Rauf, B. Akram, M. Ishtiaq, and M. K. Siddiqui, "Topological properties of curcumin and hyaluronic acid conjugated molecular structure: An anti-cancer drug," *Polycycl. Aromat. Compd.,* pp. 1–14 (2021).

[28] P. Ali, S. A. K. Kirmani, O. A. Rugaie, and F. Azam, "Degree-based topological indices and polynomials of hyaluronic acid-curcumin conjugates," *Saudi Pharm. J.*, vol. 28, no. 9, pp. 1093–1100 (2020).

[29] S. Mondal, N. De, and A. Pal, "Topological indices of some chemical structures applied for the treatment of COVID-19 patients," *Polycycl. Aromat. Compd.*, vol. 42, no. 4, pp. 1220–1234 (2022).

[30] J. B. Liu, M. Arockiaraj, M. Arulperumjothi, and S. Prabhu, "Distance-based and bond additive topological indices of certain repurposed antiviral drug compounds tested for treating COVID-19," *Int. J. Quantum Chem.*, vol. 121, no. 10, p. e26617 (2021).

[31] S. A. K. Kirmani and P. Ali, "CoM-polynomial and topological coindices of hyaluronic acid conjugates," *Arab. J. Chem.,* vol. 15, p. 103911 (2022).

[32] S. A. K. Kirmani, P. Ali, and J. Ahmad, "Topological coindices and quantitative structure-property analysis of antiviral drugs investigated in the treatment of COVID-19," *Hindawi J. Chem.*, vol. 2022, p. 3036655, 15 pages (2022).

[33] I. Gutman, "Geometric approach to degree-based topological indices: Sombor indices," *MATCH Commun. Math. Comput. Chem.*, vol. 86, pp. 11–16 (2021).

[34] V. R. Kulli and I. Gutman, "Computation of Sombor indices of certain networks," *SSRG Int. J. Appl. Chem.,* vol. 8, pp. 1–5 (2021).

[35] R. Todeschini and V. Consonni, "New local vertex invariants and molecular descriptors based on functions of the vertex degrees," *MATCH Commun. Math. Comput. Chem.*, vol. 64, no. 2, pp. 359–372 (2010).

[36] H. Lio, "Multiplicative Sombor index of graphs," *Discrete Math. Lett.,* vol. 9, pp. 80–85 (2022).

[37] V. R. Kulli, "Multiplicative Sombor indices of certain nanotubes," *Int. J. Math. Arch.,* vol. 12, no. 3, pp. 1–5 (2021).

[38] I. Radžeporić, "Chemical applicability of Sombor indices," *J. Serb. Chem. Soc.,* vol. 86, no. 5, pp. 445–457 (2021).

[39] H. Liu, H. Chen, Q. Xiao, X. Fang, and Z. Tang, "More on Sombor indices of chemical graphs and their applications to the boiling point of benzenoid hydrocarbons," *Int. J. Quantum Chem.*, vol. 121, no. 17, p. e26689 (2021).

[40] H. Deng, Z. Tang, and R. Wu, "Molecular trees with extremal values of Sombor indices," *Int. J. Quantum Chem.*, vol. 121, p. e26622 (2021).

[41] H. Liu, L. You, and Y. Huang, "Ordering chemical graphs by Sombor indices and its applications," *MATCH Commun. Math. Comput. Chem.*, vol. 87, pp. 5-22 (2022).

[42] F. Movahedi and M. H. Akhbari, "Degree-based topological indices of the molecular structure of hyaluronic acid-methotrexate conjugates in cancer treatment," *Int. J. Quantum Chem.*, vol. 123, p. e27106 (2023).

[43] S. Alikhani and N. Ghanbari, "Sombor index of polymers," *MATCH Commun. Math. Comput. Chem.*, vol. 86, pp. 715–728 (2021).

[44] H. Liu, L. You, Z. Tang, and J. B. Liu, "On the reduced Sombor index and its applications," *MATCH Commun. Math. Comput. Chem.*, vol. 86, pp. 729–753 (2021).

[45] Z. Samiei and F. Movahedi, "Investigating graph invariants for predicting properties of chemical structures of antiviral drugs," *Polycycl. Aromat. Compd.*, vol. 44, no. 10, pp. 6696-6713 (2023).

[46] Z. Samiei and F. Movahedi, "Some degree-based topological indices of the molecular structure of drugs in the treatment of RNA-viruses," *J. Inf. Optim. Sci.*, pp. 1-22 (2025). DOI: 10.47974/JIOS-1516.

[47] A. Ahmad, M. F. Nadeem, K. Elahi, and R. Hasni, "Computing topological indices of chemical structures of the conductive 2D MOFs," *J. Inf. Optim. Sci.*, vol. 42, no. 3, pp. 563–578 (2020). DOI: 10.1080/02522667.2020.1773021.

[48] F. Asif, Z. Zahid, M. N. Husin, M. Cancan, Z. Taş, M. Alaeiyan, and M. R. Farahani, "On Sombor indices of line graph of silicate carbide Si_2C_3-I[p,q]," *J. Discrete Math. Sci. Cryptogr.*, vol. 25, no. 1, pp. 301–310 (2022). DOI: 10.1080/09720510.2022.2043621.

[49] X. Zhang, F. He, K. Xiang, J. Zhang, M. Xu, P. Long, H. Su, Z. Gan, and Q. Yu, "CD44-targeted facile enzymatic activatable chitosan nanoparticles for efficient antitumor therapy and reversal of multidrug resistance," *Biomacromolecules*, vol. 19, no. 3, pp. 883–895 (2018).

[50] F. Dosio, S. Arpicco, B. Stella, and E. Fattal, "Hyaluronic acid for anticancer drug and nucleic acid delivery," *Adv. Drug Deliv. Rev.*, vol. 97, pp. 204–236 (2016).

[51] E. Kwong, J. Higgins, and A. C. Templeton, "Strategies for bringing drug delivery tools into discovery," *Int. J. Pharm.*, vol. 412, pp. 1–7 (2011). DOI: 10.1016/j.ijpharm.2011.03.024.

[52] R. Thirumalaisamy, V. Aroulmoji, M. N. Iqbal, S. Saride, M. Bhuvaneswari, M. Deepa, C. Sivasankar, and R. Khan, "Molecular insights of hyaluronic acid-ethambutol and hyaluronic acid-isoniazid drug conjugates act as promising novel drugs for the treatment of tuberculosis," *J. Biomol. Struct. Dyn.* (2022).

[53] N. S. Munjal, R. Shukla, and T. Raj Singh, "Physicochemical characterization of paclitaxel prodrugs with cytochrome 3A4 to correlate solubility and bioavailability implementing molecular docking and simulation studies," *J. Biomol. Struct. Dyn.*, vol. 40, no. 13, pp. 5983–5995, 2022.

[54] Y. Zhong, K. Goltsche, L. Cheng, F. Xie, F. Meng, C. Deng, Z. Zhong, and R. Haag, "Hyaluronic acid-shelled acid-activatable paclitaxel prodrug micelles effectively target and treat CD44-overexpressing human breast tumor xenografts in vivo," *Biomaterials,* vol. 84, pp. 250–261 (2016).

[55] C. E. Galer, D. Sano, S. C. Ghosh, J. H. Hah, E. Auzenne, A. N. Hamir, J. N. Myers, and J. Klostergaard, "Hyaluronic acid–paclitaxel conjugate inhibits growth of human squamous cell carcinomas of the head and neck via a hyaluronic acid-mediated mechanism," *Oral Oncol*., vol. 47 (2011).

[56] G. Tripodo, A. Trapani, M. L. Torre, G. Giammona, G. Trapani, and D. Mandracchia, "Hyaluronic acid and its derivatives in drug delivery and imaging: recent advances and challenges," *Eur. J. Pharm. Biopharm.*, vol. 97, pp. 400–416 (2015).

[57] E. Estrada and E. Uriarte, "Recent advances on the role of topological indices in drug discovery research," *Curr. Med. Chem.*, vol. 8, no. 13, pp. 1573–1588 (2001).

Received July, 2024